Ion motion in SiO_2 melt

1999 J. Phys.: Condens. Matter 11 5429

(http://iopscience.iop.org/0953-8984/11/28/304)

J. Phys.: Condens. Matter **11** (1999) 5429–5436. Printed in the UK PII: S0953-8984(99)01335-1

Ion motion in SiO_2 melt

Shi Ping Huang†, F Yoshida‡, Jinglin You†, Guochang Jiang† and Kuangdi Xu†

† Shanghai Enhanced Laboratory of Ferrometallurgy, Shanghai University, Shanghai 200072, People's Republic of China

‡ Department of Physics, Shiga University of Medical Science, Otsu, Shiga 520-21, Japan

Received 27 January 1999, in final form 4 May 1999

Abstract. Dynamical properties of ions are studied in SiO_2 melt by using the molecular dynamics method. The diffusion constant, ionic conductivity and velocity autocorrelation function are calculated at various pressures and temperatures. It is found that the simulated ionic conductivities are close to experimental values, and show an increase with temperature. Diffusion constants become maximum around 10 GPa, in close relation with a marked shift in the coordination number of the Si ion. The velocity autocorrelation function and its spectra are calculated by using the memory function method. These compare well with the molecular dynamics results. Discussion is given on the pressure dependence of dynamical quantities.

1. Introduction

Recently Tsuneyki *et al* have developed a two-body potential model (TTAM) by fitting the energy surfaces of the tetrahedral SiO_4 cluster, which is calculated from *ab initio* Hartree–Fock self-consistent field calculations [1]. This potential model in the molecular dynamics (MD) calculation could reproduce reasonably well the cell parameters and bulk moduli of various polymorphs of SiO_2 and describe accurately the pressure-induced crystalline-to-amorphous transition [2]. Recent lattice dynamics calculations on various polymorphs of SiO_2 have also indicated that the results based on this potential are in good agreement with the observed Raman and IR spectroscopic data [3]. In addition, the structure and properties of SiO_2 glass have been studied successfully by using this potential.

The molecular dynamics (MD) method is very useful to directly interpret dynamic processes for simple liquids. Several authors have applied this method to investigate the structural and dynamical properties of silicate liquid and glass [4]. Their results indicate that changes of bond-length and bond-angle responding to pressure and temperature variations compare well with experimental and theoretical studies, and they predict the second-order thermodynamics properties (C_v, α, β) of the system [5].

In this paper we make a detailed study of the ionic motions in SiO_2 melt. Adopting the TTAM model potential, we perform the molecular dynamics simulation to obtain diffusion constants, ionic conductivity and velocity autocorrelation functions at pressure up to 40 GPa and temperature from 2000 to 4500 K. An anomalous pressure dependence of the diffusion constants is discussed in relation to a change of the coordination number of the Si ion. The pressure dependence of the velocity autocorrelation functions (VAFs) is investigated systematically by the memory function method. Characteristic frequencies are calculated by using the MD result of partial correlation functions, and a simplified time dependence is

0953-8984/99/285429+08$30.00

assumed for the memory function. The pressure dependence is discussed by comparing the calculated VAF with the MD result.

2. Calculation

2.1. Details of the molecular dynamics simulation

The TTAM model potential adopted in our simulation takes the form [2]

$$\phi_{ij}(r) = q_i q_j / r_{ij} + f_0(b_i + b_j)\exp[(a_i + a_j - r_{ij})/(b_i + b_j)] - C_{ij}/r_{ij}^6 \qquad (1)$$

as the interaction energy between two ions of the i and j species, with $i, j = 1$ or 2 for O or Si ion, respectively. It consists both of the long-range Coulomb and the short-range repulsive interaction. In the above equation r is the distance between the two ions, q_i (q_j) is the electric charge of the ion of the i (j) species, and the parameters involved in equation (1) are listed in table 1.

Table 1. Potential parameters for the MD run [2].

	q/e	a (Å)	b (Å)	(kcal Å^6 mol^{-1})
O	−1.2	2.05	0.176	$C_{OO} = 4956$
Si	2.4	0.86	0.033	$C_{OSi} = 1633$

The molecular dynamics simulation was performed on a system of 324 ions (216 O and 108 Si), and the initial ionic position was chosen randomly in a cubic box. We have adopted the periodic truncated octahedral (PTO) and the Ewald method for the summation of the electrostatic interaction, with the time step $\Delta t = 0.001$ ps. The temperature is controlled to 5000 K for an initial 2000 steps, and after that it is reduced to what we needed (2000 K). In the constant pressure simulation, we decrease the relaxation time: the initial approach to the corrected volume for the required pressure can be sped up. The mean square displacement, the correlation function and a histogram of the coordination number of silicon are obtained by this procedure, but the volume fluctuations affect the calculation of the correlation function in the constant pressure simulation. To obtain sufficient accuracy, we first use the constant pressure simulation to measure the volume, and then measure the correlation function in a constant volume run. All simulations are performed on a DEC-500au workstation.

2.2. Transport coefficients and velocity autocorrelation function

The static conductivity can be obtained from the changes of mean squared dipole moment due to the displacement of ions. It is defined by [6]

$$\langle \Delta M(t)^2 \rangle = \left\langle \left| \sum_{i,k} (q_i \Delta r_i^+(t) - q_k \Delta r_k^-(t)) \right|^2 \right\rangle \qquad (2)$$

where $\Delta r_i^+(t) = r_i^+(t) - r_i^+(0)$ is the displacement of the ion during the time interval t, and the angular bracket stands for the equilibrium ensemble average. The static conductivity $\sigma(0)$ can be evaluated from the slope of the linear part of $\langle \Delta M(t)^2 \rangle$ in a long time run as follows

$$\sigma(0) = \lim_{t\to\infty} \frac{1}{6k_B T V_0} \frac{\langle \Delta M(t)^2 \rangle}{t} \qquad (3)$$

where V_0 and T are the volume and the temperature of the system, respectively, and k_B is the Boltzmann constant.

The velocity autocorrelation function $C_j(t)$ for the j species is defined by [7]

$$C_j(t) = \langle v_j(t)v_j(0)\rangle / \langle v_j(0)^2\rangle. \tag{4}$$

It is normalized at $t = 0$ or $C_j(0) = 1$ by definition, and $C_j(-t) = C_j(t)$. The spectrum of $C_j(t)$ is obtained by the Fourier transformation

$$C_j(\omega) = (1/2\pi)\int_{\infty}^{\infty} \mathrm{d}t \exp(\mathrm{i}\omega t)C_j(t) \tag{5}$$

which is non-negative according to the Wiener–Khinchin theorem [8]. For simplicity we denote the Fourier transformation of the function $C_j(t)$ as $C_j(\omega)$, and the similar notation $C_j(z)$ is used below for its Laplace transformation. The memory function method [9] enables us to describe $C_j(z)$ in terms of the Laplace transformation of a memory function $M_j(t)$ as

$$C_j(z) = \int_0^{\infty} \mathrm{d}t \exp(-zt)C_j(t) = 1/[z + M_j(z)]. \tag{6}$$

The spectrum $C_j(\omega)$ is related to the real part of $C_j(z = \mathrm{i}\omega)$ as

$$C_j(\omega) = (1/2\pi)\mathrm{Re}\,[C_j(z = \mathrm{i}\omega)]. \tag{7}$$

Using equations (6) and (7), $C_j(t)$ can be obtained *via* the inverse Fourier transformation of $C_j(\omega)$ when the memory function is specified. It is useful to assume the following form for $M_j(t)$

$$M_j(t) = \omega_{j1}^2 \exp(-t/\tau_1) + \omega_{j2}^2 \exp(-t/\tau_2) + At^2 \exp(-t/\tau_3) \tag{8}$$

in which, τ_1, τ_2, τ_3 and A are constants to be determined [10]. The quantities ω_{j1} and ω_{j2} represent the contribution of cations and anions to the Einstein frequency ω_j respectively [7]. These are given by

$$\omega_j^2 = (1/m_j)\langle(\partial/\partial r_j\ \partial/\partial r_j)V\rangle = \omega_{j1}^2 + \omega_{j2}^2 \tag{9}$$

$$\omega_{jk}^2 = (n_k/3m_j)\int \mathrm{d}r\, g_{jk}(r)\{\mathrm{d}^2\nu_{jk}(r)/\mathrm{d}r^2 + (2/r)\,\mathrm{d}\nu_{jk}(r)/\mathrm{d}r\}. \tag{10}$$

In equation (9) V is the total interaction energy of the system. In equation (10) $g_{jk}(r)$ is the partial correlation function between ions of the j and k species, and n_k is the number density of species k. In equation (8) the first two terms assume the distinct difference the contributions of Si and O ions in the relaxation of effective fields at short times. The third term represents enhanced correlation at intermediate times, and this phenomenological description is assumed for the present purpose. If $A = 0$, $C_j(t)$ reduce to a generalized version [11] of the result due to Berne *et al* under a certain condition [7, 10, 12], the self-diffusion constant D_j is related to $C_j(t)$ or $C_j(\omega)$ through

$$D_j = (k_BT/m_j)\int_0^{\infty} \mathrm{d}t\, C_j(t) = (k_BT\pi/m_j)C_j(\omega = 0). \tag{11}$$

It follows from equations (6), (7) and (11),

$$\omega_{j1}^2\tau_1 + \omega_{j2}^2\tau_2 + 2A\tau_3^3 = k_BT/m_jD_j. \tag{12}$$

This is the condition for the parameters in $M_j(t)$ when the right-hand side is given.

3. Results and discussion

The specific electrical conductivity calculated by means of MD simulation at different temperatures is shown in figure 1. For SiO_2 melt, there is partial covalent interaction between Si and O ion, and therefore the specific electrical conductivity is low ($\sim 10^{-5}\ \Omega^{-1}\ cm^{-1}$) near the melting point. Figure 1 presents the specific electrical conductivity, both experimental data [13] and MD simulation results. One can see that simulated ionic conductivity is close to the experimental value and shows an increase with increasing temperature. We include this comparison with experiment for specific electrical conductivity as evidence that this potential model is adequate to describe the main features of transport in SiO_2 melt.

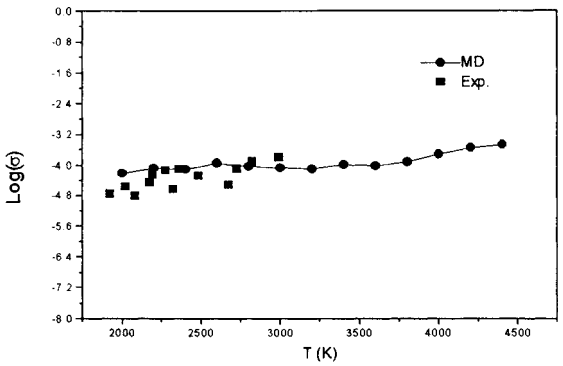

Figure 1. Comparison of specific electrical conductivity from MD simulation and experimental data at 0.1 MPa.

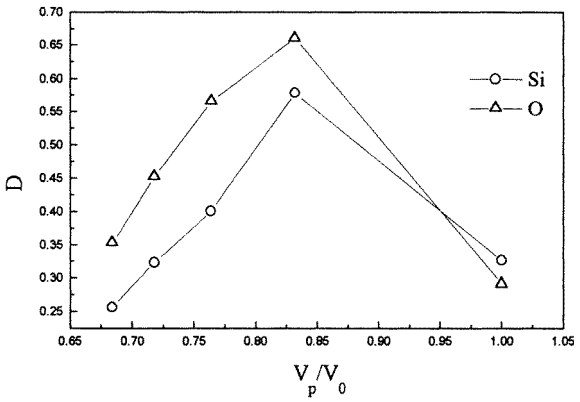

Figure 2. The self-diffusion coefficient at various compression ratios. The unit of D is $10^{-6}\ cm^2\ s^{-1}$.

The self-diffusion coefficients are estimated by the mean square displacement which runs over 20 ps. Figure 2 shows the results of the self-diffusion coefficient as a function of the compression ratio (V_p/V_0) at constant temperature (2000 K), in which V_p is the volume at pressure P (P = 0, 10, 20, 30, 40 GPa). We note that the diffusion constants of Si and O at $V_p/V_0 = 1.0$ reasonably agree with experimental results of $(CaO)_{1-x}$–$(SiO_2)_x$ melts at 1800 K. (The mole fraction $x = 0.634$, $D_{Si} = 0.34\times10^{-6}\ cm^2\ s^{-1}$, $D_0 = 0.35\times10^{-6}\ cm^2\ s^{-1}$ [14].) The results of molecular dynamics simulation show that the diffusivity of Si and O ions increases with increasing pressure from 0 to 10 GPa, and then decreases beyond it. This is consistent with the negative pressure dependence of the viscosity in silicate liquid [15], and the pressure enhancement of the ion mobility in liquid silicates [16]. As pressure increases, the coordination number certainly changes. The distribution of N_{Si-O} (the coordination number of O ions around the Si ion) is calculated for 4000 configurations by taking the first minimum in

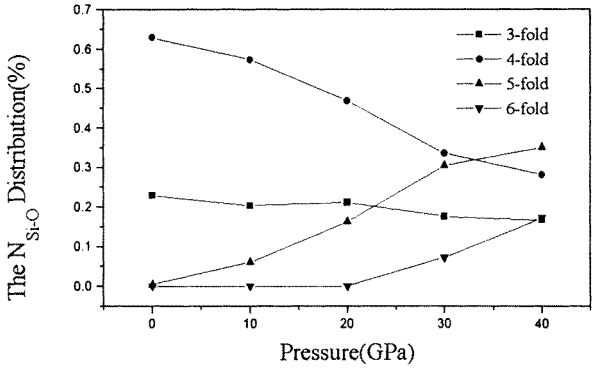

Figure 3. Pressure dependence of N_{Si-O} distribution.

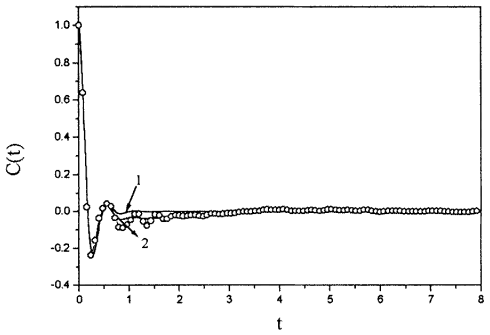

Figure 4. Velocity autocorrelation function for Si ion at $V_p/V_0 = 1.0$. Curve 1 shows the results obtained without A, and curve 2 with A in equation (8). The MD results are represented by open circles. The horizontal axis is t in the unit of 10^{-13} s.

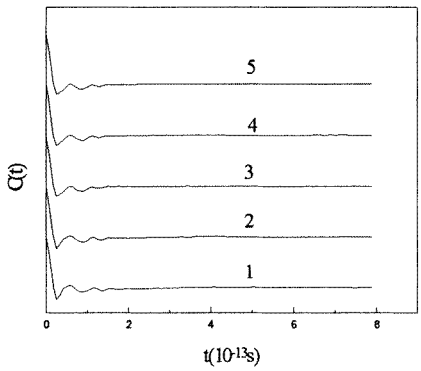

Figure 5. Velocity autocorrelation function for Si ion. The five curves show the MD results at compression ratio $V_p/V_0 = 1.0$ (curve 1), 0.823 (curve 2), 0.764 (curve 2), 0.715 (curve 4), 0.684 (curve 5).

the radial distribution function $g_{Si-O}(r)$ as a cut-off distance for the first coordination sphere. Figure 3 shows the result for N_{Si-O} (= 3, 4, 5, 6) as a function of pressure. The percentage of fivefold and sixfold coordinated Si increases rapidly with pressure from 10 to 40 GPa, but the fourfold coordinated Si decreases. When the pressure is 40 GPa, the fivefold coordinated Si becomes dominant in SiO_2 melt. These results are consistent with the NMR study on $Na_2Si_4O_9$ glass under high pressure, indicating that there are large amounts of fivefold and sixfold coordinated Si species [17].

In the range of the compression ratio V_p/V_0 from 1.0 to 0.823, the self-diffusion coefficients increase because the network structure in the SiO_2 melt is only partly broken down. Above 10 GPa, the self-diffusion coefficients decrease because the Si ion has become fivefold and sixfold coordinated and it is more tightly bound within its primary coordination shell. Recently Angell *et al* have suggested that the pressure enhancement of ion mobility in liquid silicates is correlated with a prevalence of fivefold coordination of silicon ions [6]. Figures 2 and 3 indicate that the anomalous pressure dependence of diffusion coefficient for SiO_2 melt involves not only the percentage changes of five-coordinated Si, but also three-coordinated Si.

The molecular dynamics simulation result of the velocity autocorrelation function $C_{Si}(t)$, at $V_p/V_0 = 1.00$, is shown in figure 4 as the open circles. The curve 1 shows the result of adopting equation (8) without the third term (i.e., $A = 0$). Since ω_{SiSi} is very small compared with ω_{SiO}, the value of τ_2 turns out to be very large, and as a consequence a negative tail

appears. When the third term ($A \neq 0$) is introduced in equation (8), the agreement with the MD result is improved, as shown by curve 2. It is the best obtained by following the standard procedure; we have first made a rough estimate of the parameter with some conditions with which the first minimum is reasonably reproduced. After that we have minimized the standard deviation for small variation around it, taking account of equation (12) with the MD result of the self- diffusion coefficient D_j as the condition for the parameters.

Figure 5 shows five curves of $C_{Si}(t)$ as a function of time at various compression ratios. The initial decay of velocity autocorrelation function is almost determined by the frequency ω_{Si-O}, but the subsequent behaviour is governed by the time-dependence $At^2 \exp(-t/\tau_3)$ term in the memory function. The negative region in the velocity autocorrelation function for dense liquid is understood as rebounding of particles' motion from the cage formed by surrounding particles. When a tagged particle is given an initial momentum, it comes into collision frequently with surrounding particles forming the cage, which leads to a fast decay and a long-range oscillation in time due to the so-called backflow. Figure 6(a) displays the $M_{Si}(t)$ curve as a function of time, and figure 6(b) shows the contribution of the first term, $\omega_{SiO}^2 \exp(-t/\tau_1)$, and the third term, $At^2 \exp(-t/\tau_3)$, to $M_{Si}(t)$ at $V_p/V_0 = 1.0$. We observe fast decay from the first term and a broad bump from the third term at intermediate time.

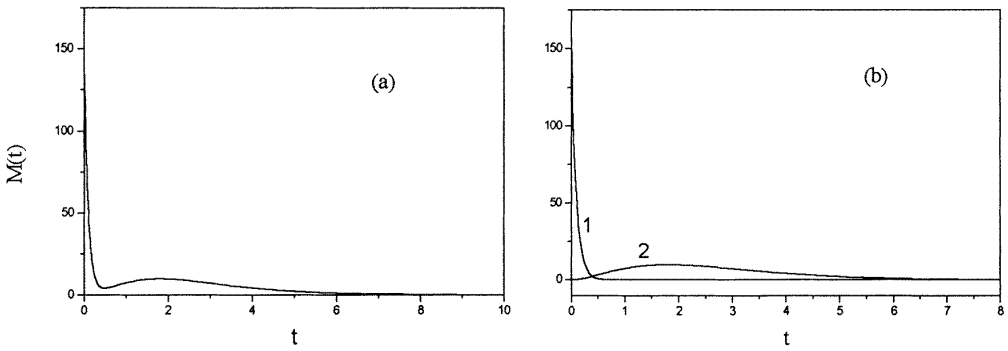

Figure 6. (a) Time dependence of the memory function $M_{Si}(t)$ given by equation (8). The unit of t is 10^{-13} s. (b) Time dependence of the first term (curve 1) and third term (curve 2) of $M_{Si}(t)$ with the same units as in (a).

Table 2. Numerical values for the parameters in equation (8) for Si ions at various compression ratios. The unit of τ_1 and τ_3 is 10^{-13} s, the unit of τ_2 is 10^{-4} s, that of ω_{SiO} is 10^{13} s^{-1}, ω_{SiSi} is 10^9 s^{-1}. A is in the unit $(10^{13}\ \text{s}^{-1})^4$.

V_p/V_0	τ_1	τ_2	τ_3	A	ω_{SiO}	ω_{SiSi}
1.000	0.0950	9.191 098	0.9000	22.500	12.5106	1.3808
0.823	0.0950	1.617 224	0.8000	20.000	12.0537	2.5661
0.764	0.0950	2.232 555	0.8500	20.500	11.8326	2.5016
0.715	0.0900	1.969 449	0.7500	20.500	11.6692	3.0263
0.684	0.0850	1.831 773	0.5000	31.500	11.6412	3.4821

The spectrum $C(\omega)$ is obtained by the Fourier transformation of $C(t)$ and is shown in figure 7. There is a high-frequency peak which comes from the contribution of ω_{Si-O}, and a low-frequency peak from the contribution of the third term. Figure 8 gives the characteristic frequencies in equation (10), evaluated by using $v_{ij}(r)$ and $g_{ij}(r)$ obtained by the molecular dynamics calculation. ω_{SiSi} is roughly three orders of magnitude smaller than ω_{SiO} (see

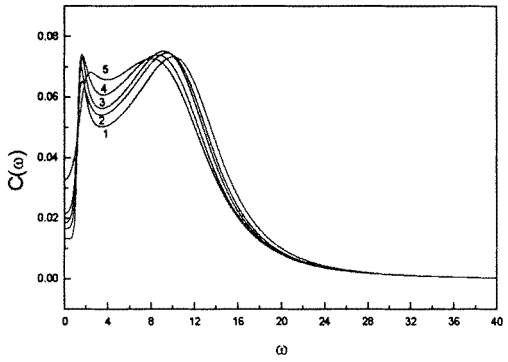

Figure 7. Spectrum of velocity autocorrelation function for Si ion at compression ratio $V_p/V_0 = 1.00$ (curve 1), 0.823 (curve 2), 0.764 (curve 3), 0.715 (curve 4), 0.684 (curve 5). The unit of ω is 10^{13} s.

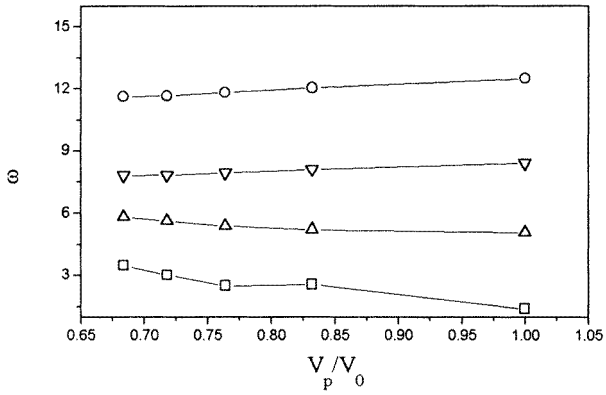

Figure 8. Compression ratio dependence of characteristic frequencies defined by equation (10): ω_{SiO} (open circles), ω_{OSi} (down triangle), ω_{OO} (up triangle), ω_{SiSi} (square). The unit of ω_{SiO}, ω_{OSi}, ω_{OO} is 10^{13} s^{-1}, but the ω_{SiSi} is 10^9 s^{-1}.

table 2). This is because the value of b_{SiSi} is very small and thus the repulsion between Si ions becomes strong. In figure 7 the spectrum tends to increase with pressure in the frequency region between the two broad peaks. If the network with the dominant fourfold Si ion partially breaks down, potential barriers around ions would significantly fluctuate in height and width. This results in broadening of characteristic frequencies for local oscillation of ions. Around 40 GPa the variation of the local field would decrease owing to tight binding characterized by the equal weight of three-, four-, fivefold Si ion. Although the characteristic frequency ω_{jk} shown in figure 8 is an averaged quantity, and it does not necessarily directly represent local variations, our results, which use this ω_{jk} in the amplitude and adopt the simplified form of the time dependence for the memory function, are consistent with the above interpretation. It would be necessary further to investigate local potential fields on ions, and also in this connection to make clear which structures (three-coordinated Si or five-coordinated Si) are responsible for the aforementioned anomalous pressure dependence of diffusion constants. Table 2 shows numerical values of parameters in equation (8) adopted for the velocity autocorrelation function in figure 5. It is found that τ_2 is much larger than τ_1, which reflects the fact that ω_{SiSi} is very much smaller than ω_{SiO}. As a consequence, in the memory function given by equation (8) for the velocity autocorrelation function, the first term, $\omega_{SiO}^2 \exp(-t/\tau_1)$, becomes dominant at short times and the third term becomes effective at intermediate times, as seen in figure 6(b).

4. Conclusion

We have investigated the self-diffusion constants and the velocity autocorrelation function to understand the ionic correlation in SiO_2 melt. The TTAM model potential is adopted for

the molecular dynamics simulation, to calculate these quantities at pressure up to 40 GPa and temperature ranging from 2000 to 4500 K. It is found in figure 2 that the self-diffusion constants take a maximum value around 10 GPa, and this behaviour is intimately related to the marked increase of the threefold and fivefold Si ion as shown in figure 3. We have evaluated the characteristic frequencies of the velocity autocorrelation function consistently by using the TTAM potential and the simulated results of the partial correlation function resulting from it, and described the time dependence in terms of the simplified memory function given in equation (8). It is found that the calculated velocity autocorrelation function is in good agreement with the molecular dynamics results, and the pressure dependence of its spectrum is roughly consistent with the structural change mentioned above.

Our results of the ionic conductivity and diffusion constants reasonably agree with experiments at $V_p/V_0 = 1.0$. This means that the TTAM potential is adequate at the starting point ($V_p/V_0 = 1.0$). We have adopted the same potential for the subsequent molecular dynamics simulation at non-zero pressure. At low pressure the local configuration around the ion would be sensitive to details of the potential. At pressure as high as 40 GPa, ions become tightly bound, as shown in the existence of three-, five- and sixfold Si ion with nearly equal weight. This situation at high pressure would not depend on details of the potential. The initial increase of calculated diffusion constants is supported by experiments. We therefore believe that if another potential is used, qualitative features of the pressure dependence would remain almost unchanged, even though quantitative changes would be substantial.

It seems to us that in order to reproduce detailed features of the velocity autocorrelation function such as the small oscillation in figure 5, it is necessary to improve the memory function. In addition, more detailed study by means of simulation is required to clarify the anomalous pressure dependence of the diffusion constants.

Acknowledgments

The authors are grateful to Dr W Smith for his excellent molecular dynamics program (DL_POLY), and two referees for their stimulative and constructive comments. This work was supported by the National Sciences Foundation of China under grant No 59874016, and the Shanghai Research Center for Advanced Materials under grant No 98JC14018.

References

[1] Tsuneyuki S *et al* 1988 *Phys. Rev. Lett.* **61** 869
[2] Tsuneyuki S *et al* 1989 *Nature* **339** 209
[3] Della Valle R G and Anderson H C 1991 *J. Chem. Phys.* **94** 5056
[4] Hemmati M and Angell C A 1997 *J. Non-Cryst. Solids* **217** 236
[5] Kubicki J D and Lasaga A C 1988 *Am. Mineral.* **73** 941
[6] Kato T *et al* 1990 *J. Chem. Phys.* **92** 5506
[7] Hansen J P and McDonald I R 1986 *The Theory of Simple Liquids* 2nd edn (London: Academic) ch 7
[8] Van Kampen N G 1981 *Stochastic Processes in Physics and Chemistry* (Amsterdam: Elsevier) ch 3
[9] Yoshida F and Takeno S 1989 *Phys. Rep.* **173** 301
[10] Hung Shi Ping and Yoshida F 1997 *J. Phys. Soc. Japan* **66** 1356
[11] Sjogren L and Yoshida F 1982 *J. Chem. Phys.* **77** 3703
[12] Berne B J, Boone J P and Rice S A 1966 *J. Chem. Phys.* **45** 1086
[13] Panish M B 1959 *J. Phys. Chem.* **63** 1337
[14] Keller H, Schwerdtfeger K, Petri H, Holzle R and Hennesn K 1982 *Metall. Trans.* B **13** 237
[15] Kushir I 1983 *Geochim. Cosmochim. Acta* **47** 1415
[16] Angell C A, Chessen P A and Tamadd S 1982 *Science* **218** 885
[17] Stebbins G J and McMillan P 1989 *Am. Mineral.* **74** 960